

Article

# A Study on the Impact of Poly(3-hexylthiophene) Chain Length and Other Applied Side-Chains on the NO<sub>2</sub> Sensing Properties of Conducting Graft Copolymers

Marcin Procek <sup>1,\*</sup> , Kinga Kepska <sup>2</sup> and Agnieszka Stolarczyk <sup>2</sup> 

<sup>1</sup> Department of Optoelectronics, Silesian University of Technology, 2 Krzywoustego Street, 44-100 Gliwice, Poland

<sup>2</sup> Department of Physical Chemistry and Technology of Polymers, Silesian University of Technology, 9 Strzody Street, 44-100 Gliwice, Poland; Kinga.Kepska@polsl.pl (K.K.); Agnieszka.Stolarczyk@polsl.pl (A.S.)

\* Correspondence: Marcin.Procek@polsl.pl; Tel.: +48-32-237-21-81

Received: 22 February 2018; Accepted: 19 March 2018; Published: 20 March 2018



**Abstract:** The detection and concentration measurements of low concentrations of nitrogen dioxide (NO<sub>2</sub>) are important because of its negative effects on human health and its application in many fields of industry and safety systems. In our approach, conducting graft copolymers based on the poly(3-hexylthiophene) (P3HT) conducting polymer and other side-chains, polyethylene glycol (PEG) and dodec-1-en, grafted on a poly(methylhydrosiloxane) backbone, were investigated. The grafts containing PEG (PEGSil) and dodec-1-en (DodecSil) in two variants, namely, fractions with shorter (hexane fraction -H) and longer (chloroform fraction -CH) side-chains of P3HT, were tested as receptor structures in NO<sub>2</sub> gas sensors. Their responses to NO<sub>2</sub>, within the concentration range of 1–20 ppm, were investigated in a nitrogen atmosphere at different operating temperatures—room temperature (RT) = 25 °C, 50 °C, and 100 °C. The results indicated that both of the copolymers with PEG side-chains had higher responses to NO<sub>2</sub> than the materials with dodec-1-en side-chains. Furthermore, the results indicated that, in both cases, H fractions were more sensitive than CH fractions. The highest response to 1 ppm of NO<sub>2</sub>, from the investigated graft copolymers, had PEGSil H, which indicated a response of 1330% at RT and 1980% at 100 °C. The calculated lower-limit of the detection of this material is lower than 300 ppb of NO<sub>2</sub> at 100 °C. This research indicated that graft copolymers of P3HT had great potential for low temperature NO<sub>2</sub> sensing, and that the proper choice of other side-chains in graft copolymers can improve their gas sensing properties.

**Keywords:** gas sensor; NO<sub>2</sub> sensor; P3HT; graft copolymers; tailor-made receptor materials; low temperature gas sensing; functionalized conducting polymers

## 1. Introduction

In the contemporary era of civilization, one of the major problems facing society is air pollution. One of the most common forms of pollution is nitrogen dioxide (NO<sub>2</sub>), which is associated with adverse effects on human health. This is because, at high concentrations, it can cause inflammation of the airways [1]. NO<sub>2</sub> also contributes to the formation of secondary particulate aerosols and tropospheric ozone (O<sub>3</sub>) in the atmosphere—both are significant air pollutants due to their adverse effects on human health [2]. Thus, NO<sub>2</sub> monitoring is important in the automotive and the energetic industries [3,4]. The nitro compounds are also components of vapors of explosive materials, such as trinitrotoluene, Research Department Explosive, and nitroglycerine [5–7].

The most popular gas sensors that are used in NO<sub>2</sub> concentration monitoring are chemoresistive gas sensors that are based on metal oxide (MOX) semiconducting receptors, such as SnO<sub>2</sub>, TiO<sub>2</sub>, ZnO, and others [8–11]. These gas sensors have many advantages, such as high sensitivity and long-term stability. However, in contrast, these materials exhibit poor selectivity and operate at relatively high temperatures (often higher than 200 °C) [12,13].

Conducting polymers (CPs) have been studied as alternative receptor materials for gas sensing since the early 1980s. Polymers—such as polyaniline, polypyrrole, polythiophene (PTh), their derivatives, and others—were studied extensively with regards to their use in gas sensors [14,15]. These materials showed some advantages, such as high sensitivity, short response times, and low operation temperatures, often room temperature (RT) [14,16]. The polymer gas sensors showed good sensing properties for NH<sub>3</sub>, NO<sub>2</sub>, I<sub>2</sub>, H<sub>2</sub>S, and volatile organic compounds (VOCs) [14,17]. CPs have been successfully applied in many types of chemical gas sensors, such as electrical (resistance, thin film transistors), mass sensitive (on surface acoustic wave and quartz crystal microbalance transducers), optical (based on surface plasmon resonance, optical fibers, fluorescence, etc.), and others [14,17–20].

Unfortunately, CPs that are in their pristine and doped form are often not able to be processed (insoluble and infusible), making such materials unattractive for mass production. For PTh, this problem was solved through functionalization, by the addition of an alkyl side-chain. These materials are named poly(alkylthiophenes) (PATs), and are soluble in many common solvents, such as chloroform, hexane, chlorobenzene, etc., making them convenient for further processing [21].

The intrinsically conducting polymers are  $\pi$ -conjugated macromolecules that show electrical and optical changes in property when they are doped/dedoped by some chemical agents. Among the  $\pi$ -conjugated polymers, poly(3-hexylthiophenes) (P3HTs) have gained particular interest because of their high mobility of charge carriers, good stability, the ability to process from a solution, and the ability to self-organize. These features are, however, the result of a number of conditions, the most important of these being the length of the polymer chain and its topology [21,22].

The major problem with the CPs applied in sensors is their fast aging processes, which make them chemically and electrically unstable in the long term [23]. Furthermore, PATs, especially regioregular (rr) ones, have poor mechanical and adhesive properties, making them more susceptible to damage [24].

The literature describes many proposed methods for improving the electrical, mechanical, and gas sensing properties of CPs. These methods include blending with other polymers, hybridization with inorganic materials (such as MOX, graphene oxide etc.), chemical modification of the polymer chain, copolymerization, and grafting, among others [17,23,25–28].

Within the scope of this paper, the objective is to develop multi-functional,  $\pi$ -conjugated materials designed to meet the demands of sensor fabrication. Observing the potential of the organic devices, we synthesized the graft copolymers of siloxane and  $\pi$ -conjugated macromolecules of rrP3HT. These materials, featuring various electron affinities, can be tailored on both a molecular and a supramolecular level, in order to exhibit a range of physicochemical properties. Therefore, our idea for a copolymer—featuring numerous degrees of freedom according to the design of its architecture—coupled with the specific properties of its constituents, will result in a new class of sensing materials.

In this paper, we report the influence of the  $\pi$ -conjugated polymer, namely the P3HT chain length, and other comonomers, such as polyelectrolyte-polyethylene glycol (PEG) and the internal plasticiser (dodec-1-en), on the NO<sub>2</sub> sensing properties of grafted comb-like copolymers with a poly(methylsiloxane) backbone. The two graft copolymers, PEGSil (Poly(dimethylsiloxane)-co-[poly(methylhydrosiloxane)-graft-2-vinyl-poly(3-hexylthiophene)]-co-[poly(methylhydrosiloxane)-graft-poly(ethylene glycol) methyl ether methacrylate]) and DodecSil (Poly(dimethylsiloxane)-co-[poly(methylhydrosiloxane)-graft-2-vinyl-poly(3-hexylthiophene)]-co-[poly(methylhydrosiloxane)-graft-dodec-1-en]), with different P3HT chain lengths, were tested as gas receptor thin films in resistance NO<sub>2</sub> sensors.

This paper presents material synthesis and characterization, a sensors fabrication process description, and a study of the NO<sub>2</sub> sensing properties of the obtained devices. Our research shows that the proper choice of CP chain length and other side-chains in graft copolymers can improve their gas sensing properties. The investigated materials show higher responses to single ppms of NO<sub>2</sub> than they do to other P3HT-based materials that are functionalized by other methods. Thus, we conclude that the grafting method appears to be a prospective way of obtaining tailor-made gas sensing materials.

## 2. Materials and Methods

The synthesis of the vinyl terminated regioregular poly(3-hexylthiophene) (vin-rrP3HT), via the Grignard Metathesis Method (GRIM) method, and the synthesis of the vinyl terminated rrP3HT, was conducted based on the procedure described in the literature in [29] (all of the materials were from Sigma Aldrich, Saint Louis, MO, USA). The polymers of two average  $M_n$ , namely, a 10,000-chloroform fraction (CH) and a 4000-hexane fraction (H)—as determined by the gel permeation chromatography (GPC) calibrated on the polystyrene standard—were prepared. The calculated average of the P3HT repeat units were 60 and 24 for the CH and H fractions, respectively. The investigated graft polymers were obtained using the method described in the patent application [30]. The synthesis was based on the grafting of the vinyl terminated P3HT with a different chain length and PEG, or dodec-1-en onto poly(methylhydrosiloxane) (PMHS) chains (all of the materials were from Sigma Aldrich, Saint Louis, MO, USA). The scheme of the synthesis of the obtained P3HT graft copolymers is presented in Figure 1.

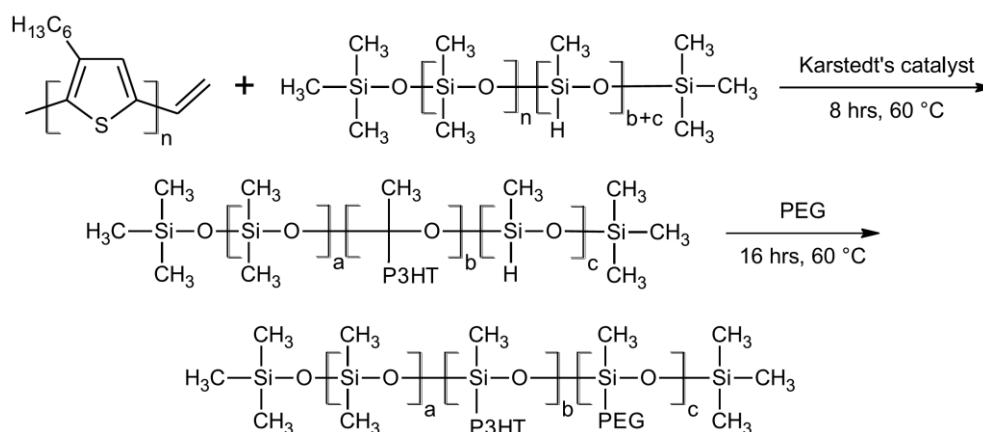


**Figure 1.** Scheme of the poly(3-hexylthiophenes) (P3HT) graft copolymer synthesis route.

The chemical structures of the investigated materials were confirmed by <sup>1</sup>H Nuclear Magnetic Resonance (<sup>1</sup>H-NMR) and Fourier-transform infrared spectroscopy with the attenuated total reflectance (FTIR-Atr). The IR spectroscopy was carried out on a Perkin-Elmer Spectrum-Two (Waltham, MA, USA) spectrometer with a Universal Attenuated Total Reflectance accessory UATR (Single Reflection Diamond) module.

An <sup>1</sup>H-NMR analysis of products was performed for solutions in CDCl<sub>3</sub> on a Varian Unity Inova (Palo Alto, CA, USA) spectrometer with a resonance frequency of 300 MHz, using tetramethylsilane (TMS) as the internal standard.

The obtained graft copolymers and polymers, which are the receptor materials, were deposited on the interdigital transducers (IDT) using spin-coating method. The IDTs with gold electrodes on the Si/SiO<sub>2</sub> substrates were described in detail in our previous works [11,18]. All of the polymers were dissolved in chloroform (CHCl<sub>3</sub>) (POCH, Gliwice, Poland) in the proportion of 2.5 mg of polymer to 1 mL of solvent. The solutions were dropped on the rotating transducers in amounts of 25 μL. During all of the coating processes, the spin rate of the IDTs were kept on a constant level of 500 rpm. Further details about the spin-coating process can be found in our previous work [18], where different graft

copolymers and pure P3HT that were obtained by the same technological process, were tested as NO<sub>2</sub> receptor materials.

The obtained sensing films were characterized using the atomic force microscopy (AFM) technique using the NTGRA Prima system (NT-MDT, Moscow, Russia) with a semi-contact mode and using HA-HR probes (NT-MDT) with a 260 kHz work frequency. The typical curative radius of the tip of the used probes is less than 10 nm, the tip length is  $\leq 1 \mu\text{m}$ , and the cantilever length is 123  $\mu\text{m}$ . All of the measurements were performed using a scanning frequency of 0.5 Hz (scan speed for  $5 \times 5 \mu\text{m}$  areas was approximately 5  $\mu\text{m/s}$ ). The AFM data were processed and analyzed using the dedicated software Nova 1.1.0.1824 (NT-MDT, Moscow, Russia).

The sensors were placed on a thick film heater on an alumina substrate and were electrically connected with chip feedthroughs using an ultrasonic wire bonding method with 25  $\mu\text{m}$  of gold wire. The temperature was controlled using a SR94 controller (Shimaden, Tokyo, Japan) with a Pt100 temperature sensor. Further details concerning the sensors' electrical connections, heating, and temperature control can be found in our previous work [11]. The four sensors (each with a different graft copolymer) were tested simultaneously using a testing chamber and mass flow controllers that were based on a measurement system that was also presented in detail in our previous work [11]. The sensors' resistance was measured using a multi-switch unit 34970A (Agilent, Santa Clara, CA, USA) within a 10 M $\Omega$  range.

The sensors' reaction to the small concentrations of NO<sub>2</sub> within the range of 1 ppm to 20 ppm, in different operating temperatures (RT = 25 °C, 50 °C, and 100 °C), were tested. The gas mixture was prepared from a calibration mixture (100 ppm NO<sub>2</sub> in N<sub>2</sub>) and a carrier gas (pure N<sub>2</sub>), using gas a dosing system that was based on the mass flow controllers. The research was conducted in a nitrogen atmosphere in order to describe the interactions of the polymeric materials with NO<sub>2</sub>, without the interference of oxygen and other reactive gases. During all of the experiments, the relative humidity (RH) of the gas mixture was kept at a constant level of  $6 \pm 1\%$ .

The sensors' responses were calculated according to the following formula:

$$\text{Response} = \frac{R_a}{R_g}, \quad (1)$$

where  $R_a$  is a base resistance in a pure carrier gas and  $R_g$  is a resistance in a target gas.

### 3. Results and Discussion

#### 3.1. Materials Characterization

Both FTIR and <sup>1</sup>H-NMR were used in order to identify and characterize the four copolymers. The assignments of the chemical shifts are presented in Table 1. The NMR has allowed for the compositional and structural determination of each copolymer. The <sup>1</sup>H-NMR spectra of the copolymer DodecSil CH and PEGSil CH, presented in Figure A1 (Appendix A), show the representative spectra for all of the copolymers that were used used (both with P3HT chain lengths).

**Table 1.** Assignments of the <sup>1</sup>H-Nuclear Molecular Resonance (NMR) of DodecSil CH and PEGSil CH signals.

Sample	<sup>1</sup> H-NMR $\delta$ (ppm)
DodecSil CH	h: 0,09 (CH <sub>3</sub> -Si-O-); g, i: 0,50 (-CH <sub>2</sub> -Si-O-) a, k: 0,91 (-CH <sub>2</sub> -CH <sub>3</sub> ); b, j: 1,34 (-CH <sub>2</sub> ) <sub>3</sub> -; c: 1,71 (-CH <sub>2</sub> -CH <sub>2</sub> -C <sub>Ar</sub> ); d: 2,80 (-CH <sub>2</sub> -C <sub>Ar</sub> ); f: 3,48 (-Si-CH <sub>2</sub> -CH <sub>2</sub> -C <sub>Ar</sub> ); e: 6,98 (H-C <sub>Ar</sub> )
PEGSil CH	h: 0,09 (CH <sub>3</sub> -Si-O-); a: 0,91 (-CH <sub>2</sub> -CH <sub>3</sub> ); b: 1,36 (-CH <sub>2</sub> ) <sub>3</sub> -; c: 1,71 (-CH <sub>2</sub> -CH <sub>2</sub> -C <sub>Ar</sub> ); d: 2,80 (-CH <sub>2</sub> -C <sub>Ar</sub> ); n: 3,38 (CH <sub>3</sub> -O-); m: 3,64 (-CH <sub>2</sub> -O-); l: 4,22 (CH <sub>2</sub> -CH <sub>2</sub> -C(=O)-); e: 6,98 (H-C <sub>Ar</sub> )

In Figure A2, the FTIR-Atr representative spectra of graft copolymers are presented. Detailed analyses of the IR signals are presented in Table 2. The spectra of the grafted copolymers, not only shows all of the characteristic peaks of the siloxane groups of Si-O-Si at  $1090\text{ cm}^{-1}$  and at  $1020\text{ cm}^{-1}$  and those of P3HT, but also shows the absorption bands of poly(ethylene glycol), such as CH<sub>2</sub> and CH<sub>3</sub>, bending at  $1467.8\text{ cm}^{-1}$  and at  $1342.4\text{ cm}^{-1}$  C–O–C. This indicates that the P3HT, poly(ethylene glycol), and dodecyl were successfully grafted onto the polysiloxane backbone.

**Table 2.** Assignments of the main Fourier-transform infrared spectroscopy with attenuated total reflectance (FTIR-Atr) features of DodecSil CH and PEGSil CH.

Sample	$\nu$ ( $\text{cm}^{-1}$ ) Assignment
DodecSil CH	794 [ $\delta^1(\text{Si}-(\text{CH}_3)_2)$ , s <sup>2</sup> ]; 1016 [ $\nu_{\text{asym.}}(\text{Si-O-Si})$ , vs]; 1260 [ $\delta_{\text{asym.}}(\text{Si-CH}_3)$ , s]; 1375 [ $\delta_{\text{sym.}}(-\text{CH}_2-)$ , w]; 1456 [ $\nu_{\text{asym.}}(\text{C}_{\text{Ar}} = \text{C}_{\text{Ar}})$ , m]; 1511 [ $\nu_{\text{sym.}}(\text{C}_{\text{Ar}} = \text{C}_{\text{Ar}})$ , w]; 2855 [ $\nu_{\text{sym.}}(\text{C-H})$ , s]; 2923 [ $\nu_{\text{asym.}}(\text{C-H})$ , vs]; 2957 [ $\nu_{\text{sym.}}(\text{C-H})$ , s]; 3056 [ $\nu(\text{C}_{\text{Ar}}-\text{H})$ , w]
PEGSil CH	795 [ $\delta(\text{Si}-(\text{CH}_3)_2)$ , s]; 1022 [ $\nu_{\text{asym.}}(\text{Si-O-Si})$ , vs]; 1260 [ $\delta_{\text{asym.}}(\text{Si-CH}_3)$ , s]; 1379 [ $\delta_{\text{sym.}}(-\text{CH}_2-)$ , w]; 1456 [ $\nu_{\text{asym.}}(\text{C}_{\text{Ar}} = \text{C}_{\text{Ar}})$ , m]; 1508 [ $\nu_{\text{sym.}}(\text{C}_{\text{Ar}} = \text{C}_{\text{Ar}})$ , w]; 1735 [ $\nu(\text{C}=\text{O})$ , w]; 2853 [ $\nu_{\text{sym.}}(\text{C-H})$ , s]; 2926 [ $\nu_{\text{asym.}}(\text{C-H})$ , vs]; 2952 [ $\nu_{\text{sym.}}(\text{C-H})$ , s]; 3055 [ $\nu(\text{C}_{\text{Ar}}-\text{H})$ , w]

<sup>1</sup> vibration type:  $\nu$ —stretching;  $\delta$ —deformation; sym.—symetric; asym.—asymmetric; <sup>2</sup> band intensity: w—weak; m—medium; s—strong; vs—very strong.

The morphology of all of the prepared polymer sensing films was investigated using the AFM method. These measurements showed that all of the films were homogenous and smooth, with root mean squares (RMS) smaller than 2 nm (Table 3). Since all of the results were similar, the representative AFM height of the images (of  $5 \times 5\ \mu\text{m}$  areas between the IDT electrodes) has been presented in Figure 2 (the complementary phase images are presented in Figure A3). The thickness of all of the films were measured using the AFM method and found to be approximately  $20 \pm 5\text{ nm}$ . The base resistance of the sensing structures measured at RT in pure N<sub>2</sub> are presented in Table 3.

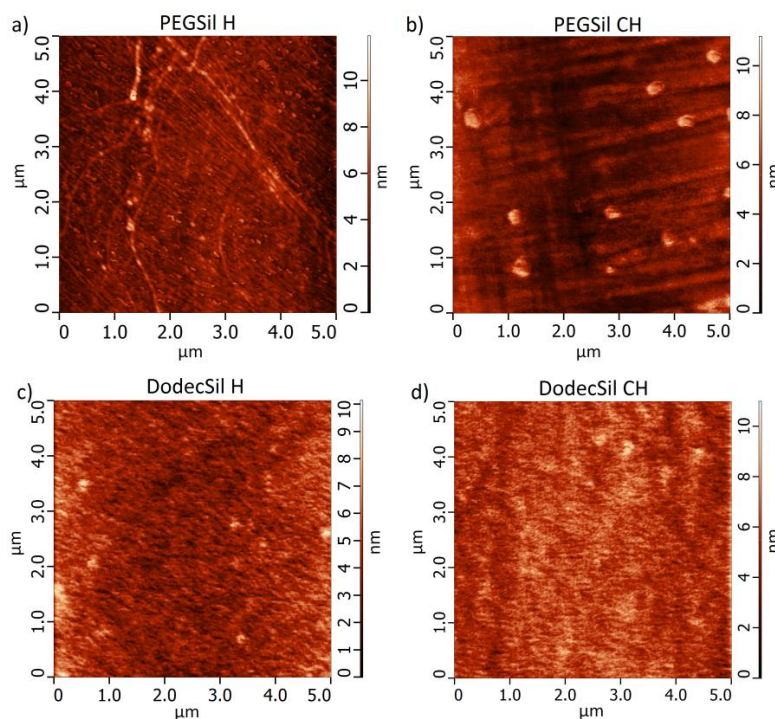


**Figure 2.** Atomic force microscopy (AFM) height images from  $5 \times 5\ \mu\text{m}$  areas between the electrodes of (a) PEGSil H; (b) PEGSil CH; (c) DodecSil H; (d) DodecSilCH.



**Table 3.** Root mean square (RMS) roughness values calculated from  $5 \times 5 \mu\text{m}$  areas between the electrodes and base resistance at room temperature (RT) in  $\text{N}_2$  for all sensing structures.

Sample	PEGSil H	PEGSil CH	DodecSil H	DodecSil CH
RMS ( $5 \times 5 \mu\text{m}$ ), nm	$1.24 \pm 0.20$	$1.21 \pm 0.20$	$1.05 \pm 0.10$	$1.06 \pm 0.10$
Base Resistance, k $\Omega$	$1087.5 \pm 1.0$	$128.7 \pm 1.0$	$18496.4 \pm 1.0$	$113.3 \pm 1.0$

### 3.2. Gas Sensing Measurements

The conductivity of the studied graft copolymers is provided by the presence of the CP (P3HT) chains. The application of the polymethylsiloxane backbone is responsible for the positive film forming process and adhesive properties. Additionally, siloxane has good gas permeability values and, as a result it does not significantly interfere with the gas diffusion processes in sensing films. The other side-chains, PEG or dodec-1-en, were applied to improve the mechanical properties of the investigated graft copolymers. PEG is a well-known polyelectrolyte, which increases gas and charge transfer in the sensing films. PEG has positive  $\text{NO}_x$  adsorption properties [31]. Thus, it is added to our grafts in order to improve the material sensing properties, while dodec-1-en is only the internal plasticizer and should not show additional interaction with the analyte. Thus, the addition of this comonomer will improve the mechanical properties of the sensing material.

In all cases,  $\text{NO}_2$  causes a decrease of the sensors' resistance (this is a response increase) as it is a typical p-type semiconductor reaction to the oxidizing gas action. The sensing mechanism is based on the P3HT doping process, where  $\text{NO}_2$  is an electron acceptor dopant [32,33]. The reaction of P3HT with  $\text{NO}_2$  leads to an increase in the holes of concentration, because of the formation of polarons followed by bipolaron formation [22,34].

For low concentrations of  $\text{NO}_2$  (lower than 10 ppm) at RT, polarons are generated, causing the resistance to drop, seen in Figure 3a. However, all of the investigated materials stay in their semiconducting states. After some time at higher  $\text{NO}_2$  concentrations, the polaron concentration becomes sufficient for bipolaron generation to occur. This can be seen in Figure 3a, for 10 and 20 ppm peaks, where a very fast resistance drop (response increase) to small values (even hundreds of ohms) is observed. Consequently, polymers switched to conducting states. Furthermore, the differences between the time and concentration of where bipolaron generation starts shows that CP chain length has an influence on this process [35,36]. P3HT H has a shorter effective conjugation length and prefers to generate stable polarons, in contrast to longer P3HT CH chain, where the generation of bipolarons is more probable. This leads us to conclude that, for  $\text{NO}_2$  sensing applications, the semiconducting state of P3HT is required for proper  $\text{NO}_2$  concentration measurement, and its conducting state is an upper limit for the proper operation sensors. However, it has to be stressed that the adsorption processes are reversible in all cases, after the  $\text{NO}_2$  removal sensor resistance returns to its initial value. Unfortunately, at RT, the regeneration process is slow (Figure 3a) and an operating temperature elevation is required to improve sensor dynamics.

At higher temperatures (50 °C and 100 °C), a switch to the conducting state was not observed in measured the concentration range, as seen in Figure 3b,c. Thermal activation causes faster  $\text{NO}_2$  desorption/polarons recombination. Consequently the bipolarons were not generated, the sensor operated faster, and regeneration was more efficient.

The significant differences in sensor responses were observed between graft copolymers with PEG and those with dodec-1-en side-chains. According to our prediction, PEG improved sensor responses due to the abovementioned interaction with  $\text{NO}_2$ . The sensor responses to 5 ppm of  $\text{NO}_2$  at 50 °C, shown in Figure 4a, and to 1 ppm of  $\text{NO}_2$  at different temperatures, shown in Figure 4b, are collected and shown in Figure 4 for an easy comparison. It is evident that, in all cases, PEGSils' responses were higher than those of DodecSils. Furthermore, in all cases, H fractions exhibited higher responses to  $\text{NO}_2$  than CH fractions did. The highest responses were observed at the temperature of

100 °C. In this case, the sensors showed the best stability and operation dynamics out of all the used operating temperatures.

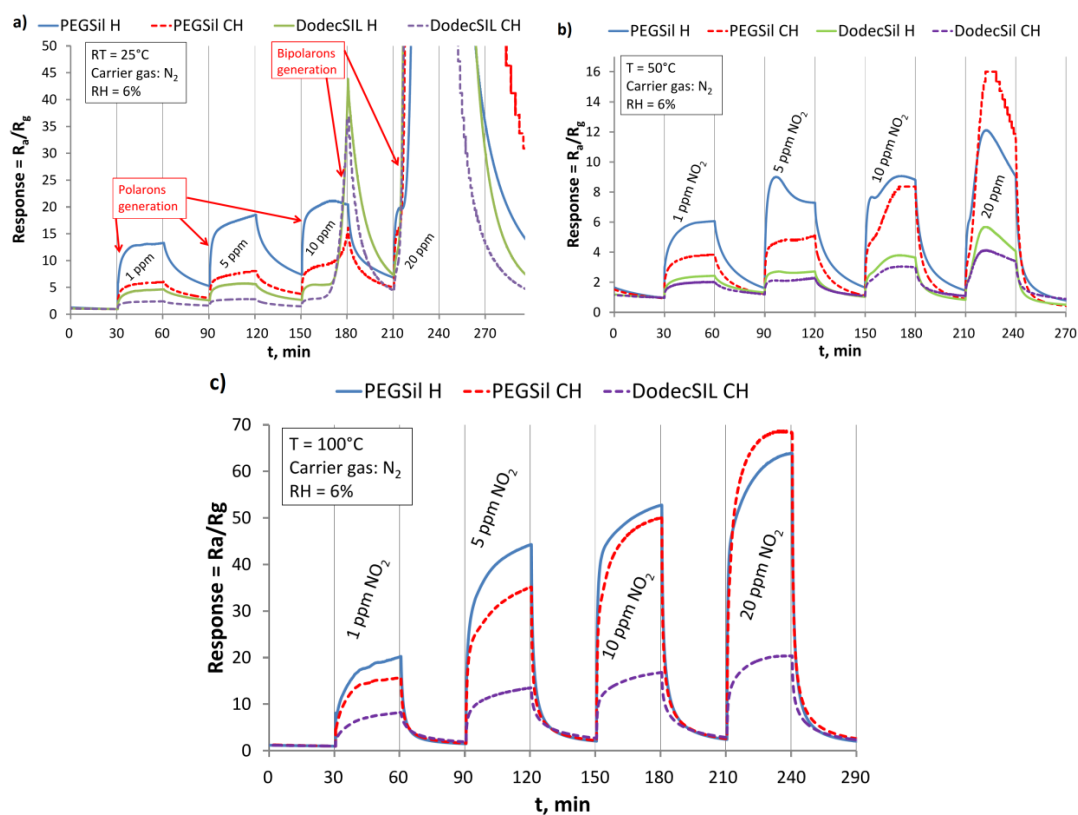


**Figure 3.** Sensor responses to different nitrogen dioxide ( $\text{NO}_2$ ) concentrations at (a)  $\text{RT} = 25\text{ }^\circ\text{C}$ ; (b)  $50\text{ }^\circ\text{C}$ ; (c)  $100\text{ }^\circ\text{C}$ .

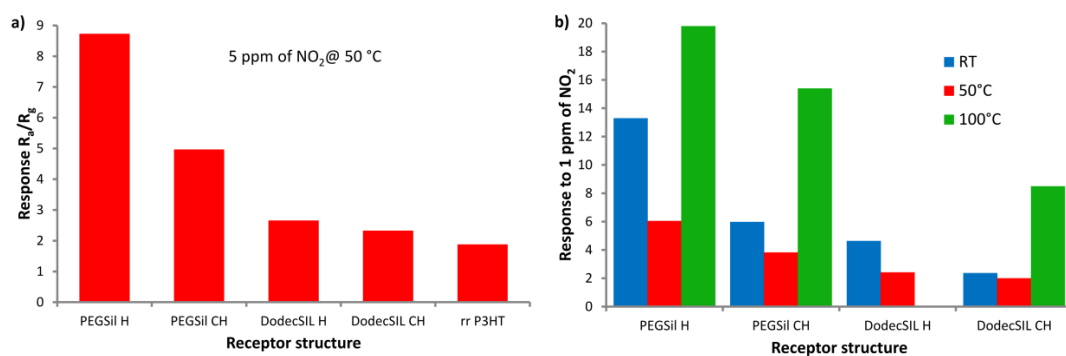


**Figure 4.** Summary of sensor responses to (a) 5 ppm of  $\text{NO}_2$  at  $50\text{ }^\circ\text{C}$ , in reference to rrP3HT response taken from our previous work [18]; (b) 1 ppm of  $\text{NO}_2$  at different temperatures.

The sensors' scalability at  $100\text{ }^\circ\text{C}$  was confirmed using the calibration curves presented in Figure 5. In this case, the gas sensors demonstrate the logarithmic dependence between the response and the concentration. In order to show the sensors' potential for low concentration detection, the calibration curves are presented in a semi-logarithmic scale with logarithmic approximations. Figure 5 shows that the proposed sensors have great potential for sub-ppm and ppb levels of  $\text{NO}_2$  concentration measurements.

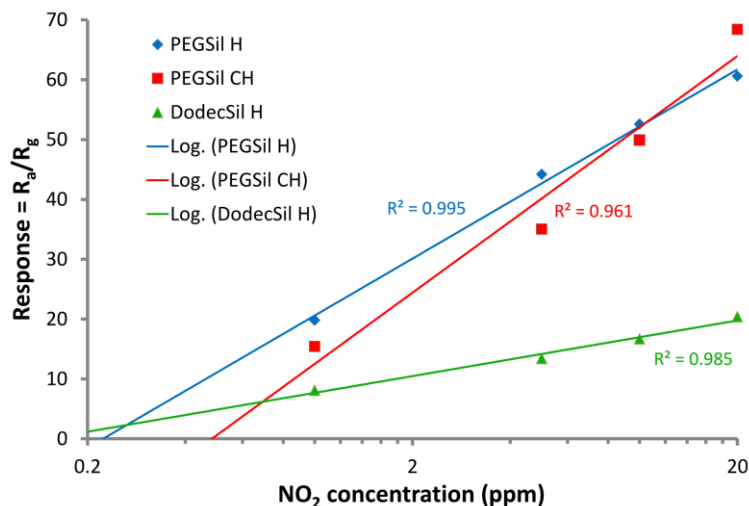


Figure 5. Sensors' calibration curves in a semi-logarithmic scale for an operating temperature = 100 °C.

Table 4 presents a comparison of the responses to NO<sub>2</sub> of PEGSil H and other P3HT-based receptor materials that were recently investigated in the literature. This summary shows that the graft copolymers investigated in our current and previous work [18] show higher responses to NO<sub>2</sub> than clean P3HT and P3HT that are functionalized using other methods. In this case, the responses to 1 ppm of NO<sub>2</sub>, at all measured temperatures were significantly higher than the responses of the other compared materials' responses to 4 ppm or 5 ppm of NO<sub>2</sub> (Table 4). This confirms that the investigated materials have a greater potential for the measuring of NO<sub>2</sub> in sub-ppm and ppb concentration levels than other P3HT-based materials. Thus, we can conclude that our strategy for improving the NO<sub>2</sub> sensing properties of CPs, using the grafting method, is a promising advance in the research of tailor-made functionalized receptor materials. The obtained results show that the responses of the proposed graft copolymers are comparable with MOX based sensors and can be considered as an alternative to these sensors for NO<sub>2</sub> sensing. The advantages of these materials include a relatively low operating temperature and the numerous technologies available for the application on transducers, (such as spin-coating, printing, drop-coating, and dip-coating methods). However, long-term stability and selectivity of such materials still require further investigation.

Table 4. Comparison of the responses of P3HT-based receptor structures to NO<sub>2</sub>.

Material	NO <sub>2</sub> Concentration	Response	Operating Temperature	Reference
PEGSil H	1 ppm	1330%	RT	Current work
		605%	50 °C	
		1980%	100 °C	
rrP3HT	5 ppm	188%	50 °C	[18]
P3HT	5 ppm	11% *	RT	[33]
Poly(methylsiloxane)-graft-poly(3-hexylthiophe)-graft-poly(ethylene glycol)	5 ppm	2300%	50 °C	[18]
(P3HT) ZnO@GO hybrid	5 ppm	210%	50 °C	[37]
P3HT/ZnO NS-NR composite	4 ppm	60% *	RT	[38]
RGO-P3HT composite	4 ppm	40% *	RT	[39]
P3HT:ZnO (ratio6:2) hybrid	5 ppm	20% *	RT	[40]
P3HT-SnO <sub>2</sub> composite	5 ppm	500%	100 °C	[41]
Poly-(bisdodecylquaterthiophene)	5 ppm	300% *	RT	[26]
poly-(bisdodecylthioquaterthiophene)	5 ppm	450% *	RT	[26]
P3HT:ZnO-nanowire composite	4 ppm	30% *	RT	[42]

\* Response calculated as  $(R_a - R_g)/R_a$  or  $(I_a - I_g)/I_a$ .



#### 4. Conclusions

In summary, this work presents the results of research on new graft copolymers that contain the semiconductor rrP3HT chain in their structures. The aim of the work was to examine the sensor's response to NO<sub>2</sub>, in order to check whether the addition of rrP3HT to the polymethylhydrosiloxane chain, and the additional grafting of various types of comonomers, would affect the rrP3HT sensor properties. Our approach shows that the proper selection of the graft copolymers, and the length of CP chains, improve the sensing properties of the polymer gas receptor material. The investigated materials show higher responses to single ppms of NO<sub>2</sub> than other P3HT-based materials (cleaned or functionalized by other methods). These responses are comparable to many MOX-based sensors and can be considered as an alternative to these sensors for NO<sub>2</sub> sensing. The advantages of the proposed grafted copolymers-based sensors include their ability to operate at a relatively low temperature and the numerous technologies available for the application of such materials on transducers. The obtained sensing structures show the potential to measure low concentrations at sub-ppm and ppb level, making them useful for many applications. Based on these results found in our research, we presented a novel alternative method of obtaining the tailor-made gas sensing materials, based on CPs.

**Acknowledgments:** Publication supported as a part of the Rector's grants in the area of scientific research and development works. Silesian University of Technology, grants numbers: 05/040/RGJ18/0022 and 04/010/RGJ18/0077. The present work was partially sponsored by the Polish National Science Centre "NCN" within the grant 2016/23/B/ST5/03103 and Silesian University of Technology, Faculty of Electrical Engineering within the grant BKM/567/Re4/2017.

**Author Contributions:** Marcin Procek designed and carried out the gas sensing experiments, designed the experiment stand, conducted sensor preparation technology processes, participated in material characterization, analyzed the data and participated in preparing the paper. Agnieszka Stolarczyk designed and dealt with the materials syntheses, participated in material characterization, analyzed the data, described sensing mechanisms and participated in preparing the paper. Kinga Kepska participated in materials syntheses and characterization.

**Conflicts of Interest:** The authors declare no conflict of interest.

#### Appendix A

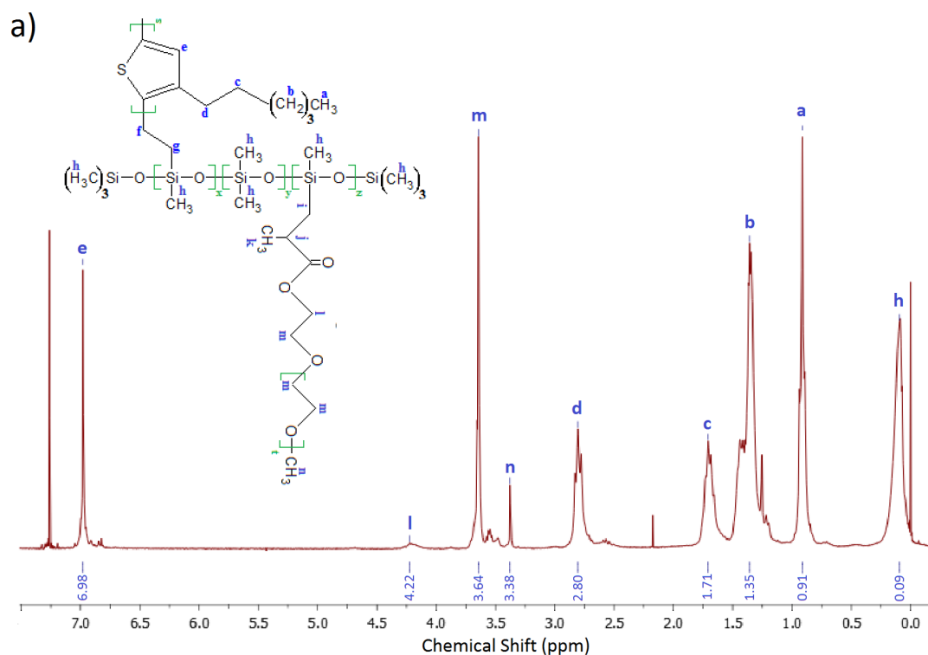
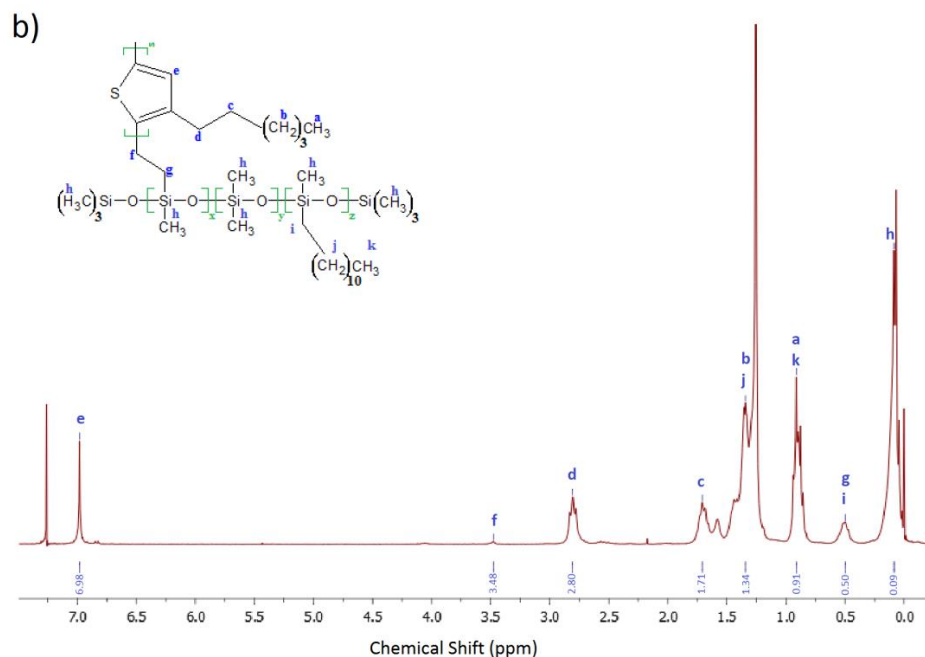
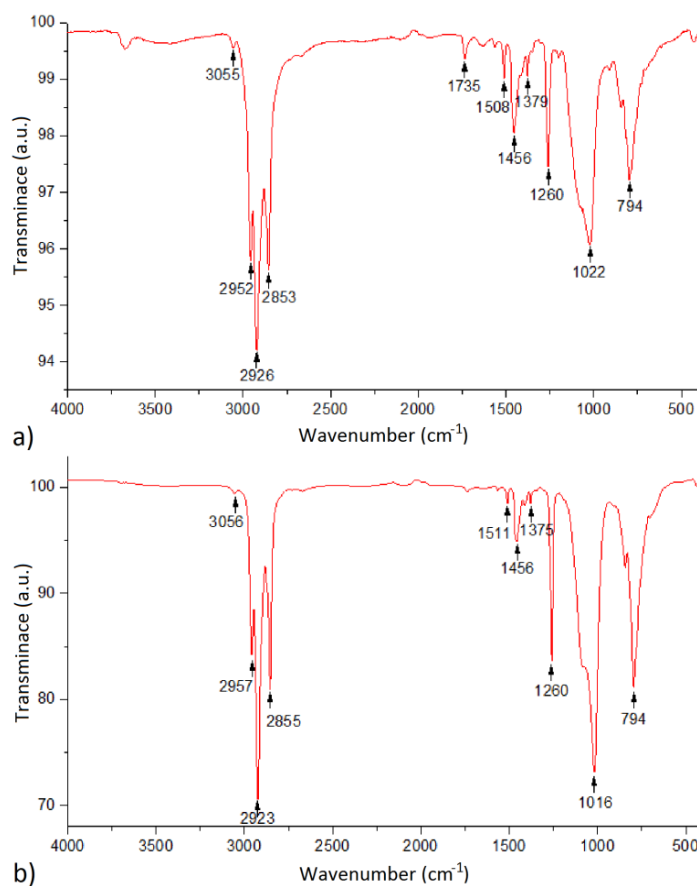


Figure A1. Cont.



**Figure A1.**  $^1\text{H}$  Nuclear Molecular Resonance ( $^1\text{H}$ -NMR) spectra of (a) PEGSil CH; (b) DodecSil CH. Marked by letters of the hydrogen atoms group assigned to particular observed signal groups visible in the  $^1\text{H}$ -NMR spectrum. Polymers' macroparticles schemes are shown in the spectrograms.



**Figure A2.** Fourier-transform infrared spectroscopy with the attenuated total reflectance (FTIR-Atr) spectra of (a) PEGSil CH; (b) DodecSil CH.

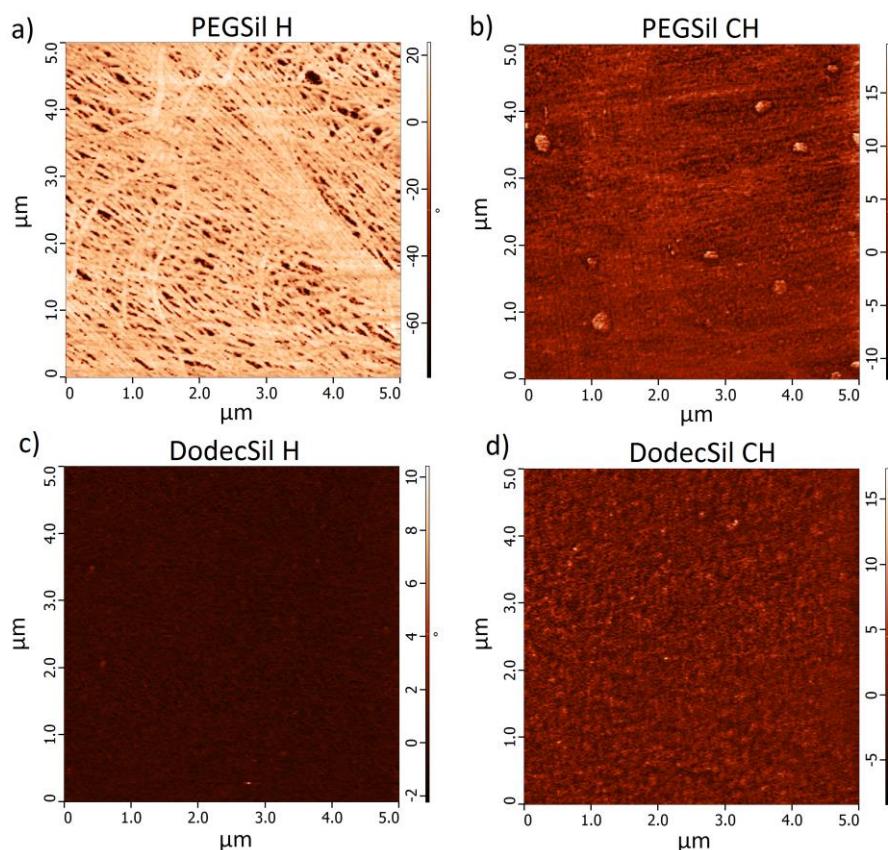


**Figure A3.** Atomic force microscopy (AFM) phase images from  $5 \times 5 \mu\text{m}$  areas between the electrodes of (a) PEGSil H; (b) PEGSil CH; (c) DodecSil H; (d) DodecSil CH.

## References

1. Kampa, M.; Castanas, E. Human health effects of air pollution. *Environ. Pollut.* **2008**, *151*, 362–367. [[CrossRef](#)] [[PubMed](#)]
2. Yoo, J.-M.; Jeong, M.-J.; Kim, D.; Stockwell, W.R.; Yang, J.-H.; Shin, H.-W.; Lee, M.-I.; Song, C.-K.; Lee, S.-D. Spatiotemporal variations of air pollutants ( $\text{O}_3$ ,  $\text{NO}_2$ ,  $\text{SO}_2$ , CO,  $\text{PM}_{10}$  and VOCs) with land-use types. *Atmos. Chem. Phys. Discuss.* **2015**, *15*, 16985–17050. [[CrossRef](#)]
3. Halfaya, Y.; Bishop, C.; Soltani, A.; Sundaram, S.; Aubry, V.; Voss, P.L.; Salvestrini, J.P.; Ougazzaden, A. Investigation of the performance of HEMT-based  $\text{NO}$ ,  $\text{NO}_2$  and  $\text{NH}_3$  exhaust gas sensors for automotive antipollution systems. *Sensors* **2016**, *16*, 273. [[CrossRef](#)] [[PubMed](#)]
4. Kim, B.-J.; Song, I.-G.; Kim, J.-S.  $\text{In}_2\text{O}_3$ -based micro gas sensor for detecting  $\text{NO}_x$  gases. *Electron. Mater. Lett.* **2014**, *10*, 509–513. [[CrossRef](#)]
5. Procek, M.; Stolarczyk, A.; Pustelny, T.; Maciak, E. A Study of a QCM Sensor Based on  $\text{TiO}_2$  Nanostructures for the Detection of  $\text{NO}_2$  and Explosives Vapours in Air. *Sensors* **2015**, *15*, 9563–9581. [[CrossRef](#)] [[PubMed](#)]
6. Bielecki, Z.; Janucki, J.; Kawalec, A.; Mikolajczyk, J.; Palka, N.; Pasternak, M.; Pustelny, T.; Stacewicz, T.; Wojtas, J. Sensors and systems for the detection of explosive devices—An overview. *Metrol. Meas. Syst.* **2012**, *19*, 3–28. [[CrossRef](#)]
7. Blue, R.; Uttamchandani, D.; Thomson, N.; Skabara, P. Novel polymer materials for low-cost nitro vapor detection sensors. In Proceedings of the 2015 IEEE Sensors, Busan, Korea, 1–4 November 2015; pp. 1–4.
8. Yunusa, Z.; Hamidon, M.N.; Kaiser, A.; Awang, Z. Gas sensors: A review. *Sens. Transducers* **2014**, *168*, 61–75.
9. Liu, X.; Cheng, S.; Liu, H.; Hu, S.; Zhang, D.; Ning, H. A Survey on Gas Sensing Technology. *Sensors* **2012**, *12*, 9635–9665. [[CrossRef](#)] [[PubMed](#)]
10. Neri, G. First Fifty Years of Chemosensitive Gas Sensors. *Chemosensors* **2015**, *3*, 1–20. [[CrossRef](#)]

11. Procek, M.; Stolarczyk, A.; Pustelny, T. Impact of Temperature and UV Irradiation on Dynamics of NO<sub>2</sub> Sensors Based on ZnO Nanostructures. *Nanomaterials* **2017**, *7*, 312. [[CrossRef](#)] [[PubMed](#)]
12. Ponzoni, A.; Baratto, C.; Cattabiani, N.; Falasconi, M.; Galstyan, V.; Nunez-Carmona, E.; Rigoni, F.; Sberveglieri, V.; Zambotti, G.; Zappa, D. Metal Oxide Gas Sensors, a Survey of Selectivity Issues Addressed at the SENSOR Lab, Brescia (Italy). *Sensors* **2017**, *17*, 714. [[CrossRef](#)] [[PubMed](#)]
13. Gardon, M.; Guilemany, J.M. A review on fabrication, sensing mechanisms and performance of metal oxide gas sensors. *J. Mater. Sci. Mater. Electron.* **2013**, *24*, 1410–1421. [[CrossRef](#)]
14. Bai, H.; Shi, G. Gas Sensors Based on Conducting Polymers. *Sensors* **2007**, *7*, 267–307. [[CrossRef](#)]
15. Miasik, J.J.; Hooper, A.; Tofield, B.C. Conducting polymer gas sensors. *J. Chem. Soc. Faraday Trans. 1 Phys. Chem. Condens. Phases* **1986**, *82*, 1117. [[CrossRef](#)]
16. Fratoddi, I.; Venditti, I.; Cametti, C.; Russo, M.V. Chemiresistive polyaniline-based gas sensors: A mini review. *Sens. Actuators B Chem.* **2015**, *220*, 534–548. [[CrossRef](#)]
17. Kumar, V.; Kim, K.-H.; Kumar, P.; Jeon, B.-H.; Kim, J.-C. Functional hybrid nanostructure materials: Advanced strategies for sensing applications toward volatile organic compounds. *Coord. Chem. Rev.* **2017**, *342*, 80–105. [[CrossRef](#)]
18. Maciak, E.; Procek, M.; Kepska, K.; Stolarczyk, A. Study of optical and electrical properties of thin films of the conducting comb-like graft copolymer of polymethylsiloxane with poly(3-hexylthiophene) and poly(ethylene glycol) side chains for low temperature NO<sub>2</sub> sensing. *Thin Solid Films* **2016**, *618*, 277–285. [[CrossRef](#)]
19. Öztürk, S.; Kösemen, A.; Şen, Z.; Kılınç, N.; Harbeck, M. Poly(3-Methylthiophene) Thin Films Deposited Electrochemically on QCMs for the Sensing of Volatile Organic Compounds. *Sensors* **2016**, *16*, 423. [[CrossRef](#)] [[PubMed](#)]
20. Stahl, U.; Voigt, A.; Dirschka, M.; Barié, N.; Richter, C.; Waldbaur, A.; Gruhl, F.; Rapp, B.; Rapp, M.; Länge, K. Long-Term Stability of Polymer-Coated Surface Transverse Wave Sensors for the Detection of Organic Solvent Vapors. *Sensors* **2017**, *17*, 2529. [[CrossRef](#)] [[PubMed](#)]
21. Inzelt, G.; Pineri, M.; Schultze, J.; Vorotyntsev, M. Electron and proton conducting polymers: Recent developments and prospects. *Electrochim. Acta* **2000**, *45*, 2403–2421. [[CrossRef](#)]
22. Lange, U.; Roznyatovskaya, N.V.; Mirsky, V.M. Conducting polymers in chemical sensors and arrays. *Anal. Chim. Acta* **2008**, *614*, 1–26. [[CrossRef](#)] [[PubMed](#)]
23. Park, S.; Park, C.; Yoon, H. Chemo-Electrical Gas Sensors Based on Conducting Polymer Hybrids. *Polymers* **2017**, *9*, 155. [[CrossRef](#)]
24. Kepska, K.; Jarosz, T.; Januszkiewicz-Kaleniak, A.; Domagala, W.; Lapkowski, M.; Stolarczyk, A. Spectroelectrochemistry of poly(3-hexylthiophenes) in solution. *Chem. Pap.* **2018**, *72*, 251–259. [[CrossRef](#)] [[PubMed](#)]
25. Han, S.; Zhuang, X.; Shi, W.; Yang, X.; Li, L.; Yu, J. Poly(3-hexylthiophene)/polystyrene (P3HT/PS) blends based organic field-effect transistor ammonia gas sensor. *Sens. Actuators B Chem.* **2016**, *225*, 10–15. [[CrossRef](#)]
26. Li, H.; Dailey, J.; Kale, T.; Besar, K.; Koehler, K.; Katz, H.E. Sensitive and Selective NO<sub>2</sub> Sensing Based on Alkyl- and Alkylthio-Thiophene Polymer Conductance and Conductance Ratio Changes from Differential Chemical Doping. *ACS Appl. Mater. Interfaces* **2017**, *9*, 20501–20507. [[CrossRef](#)] [[PubMed](#)]
27. Maciak, E.; Stolarczyk, A.; Procek, M. Surface plasmon resonance study of comb copolymers containing regioregular poly-3-hexylthiophene. In *Optical Fibers and Their Applications 2015*; Romaniuk, R.S., Wojcik, W., Smolarz, A., Eds.; SPIE—International Society for Optical Engineering: Bellingham, WA, USA, 2015.
28. Procek, M.; Stolarczyk, A.; Maciak, E. Study of the impact of UV radiation on NO<sub>2</sub> sensing properties of graft comb copolymers of poly(3-hexylthiophene) at room temperature. *Proc. SPIE Int. Soc. Opt. Eng.* **2017**, *10455*, 104550N.
29. Jeffries-El, M.; Geneviève, S.; McCullough, R.D. Facile Synthesis of End-Functionalized Regioregular Poly(3-alkylthiophene)s via Modified Grignard Metathesis Reaction. *Macromolecules* **2005**, *38*, 10346–10352. [[CrossRef](#)]
30. Stolarczyk, A.; Turczyn, R.; Januszkiewicz-Kaleniak, A.; Kepska, K. The macromolecule comb-graft polymer of polydimethylsiloxane graft-conjugated polyether and a method for its preparation. *Pol. Pat. Appl.* **2014**, *407784*, RR10.
31. Li, D.; Shi, P.; Wang, J.; Li, J.; Su, R. High-efficiency absorption of high NO<sub>x</sub> concentration in water or PEG using capillary pneumatic nebulizer packed with an expanded graphite filter. *Chem. Eng. J.* **2014**, *237*, 8–15. [[CrossRef](#)]

32. Cerion Solis, J.; De la Rosa, E.; Pena Cabrera, E. Absorption and refractive index changes of poly(3-octylthiophene) under NO<sub>2</sub> gas exposure. *Opt. Mater.* **2006**, *29*, 167–172. [[CrossRef](#)]
33. Xie, T.; Xie, G.; Du, H.; Zhou, Y.; Xie, F.; Jiang, Y.; Tai, H. The Fabrication and Optimization of Thin-Film Transistors Based on Poly(3-Hexylthiophene) Films for Nitrogen Dioxide Detection. *IEEE Sens. J.* **2016**, *16*, 1865–1871. [[CrossRef](#)]
34. Potje-Kamloth, K. Semiconductor junction gas sensors. *Chem. Rev.* **2008**, *108*, 367–399. [[CrossRef](#)] [[PubMed](#)]
35. Kroon, R.; Mengistie, D.A.; Kiefer, D.; Hynynen, J.; Ryan, J.D.; Yu, L.; Müller, C. Thermoelectric plastics: From design to synthesis, processing and structure–property relationships. *Chem. Soc. Rev.* **2016**, *45*, 6147–6164. [[CrossRef](#)] [[PubMed](#)]
36. Monteiro, F.F.; Ribeiro Junior, L.A.; de Almeida Fonseca, A.L.; e Silva, G.M.; da Cunha, W.F. Electron–phonon coupling effects on intrachain polaron recombination in conjugated polymers. *J. Mol. Model.* **2017**, *23*, 1299–1308. [[CrossRef](#)] [[PubMed](#)]
37. Wu, M.-C.; Liao, H.-C.; Lo, H.-H.; Chen, S.; Lin, Y.-Y.; Yen, W.-C.; Zeng, T.-W.; Chen, C.-W.; Chen, Y.-F.; Su, W.-F. Nanostructured polymer blends (P3HT/PMMA): Inorganic titania hybrid photovoltaic devices. *Sol. Energy Mater. Sol. Cells* **2009**, *93*, 961–965. [[CrossRef](#)]
38. Lu, F.; Cai, W.; Zhang, Y. ZnO Hierarchical Micro/Nanoarchitectures: Solvothermal Synthesis and Structurally Enhanced Photocatalytic Performance. *Adv. Funct. Mater.* **2008**, *18*, 1047–1056. [[CrossRef](#)]
39. Xie, T.; Xie, G.; Zhou, Y.; Huang, J.; Wu, M.; Jiang, Y.; Tai, H. Thin film transistors gas sensors based on reduced graphene oxide poly(3-hexylthiophene) bilayer film for nitrogen dioxide detection. *Chem. Phys. Lett.* **2014**, *614*, 275–281. [[CrossRef](#)]
40. Xie, T.; Xie, G.; Du, H.; Su, Y.; Ye, Z.; Chen, Y.; Jiang, Y. Two novel methods for evaluating the performance of OTFT gas sensors. *Sens. Actuators B Chem.* **2016**, *230*, 176–183. [[CrossRef](#)]
41. Zhao, T.; Fu, X.; Cui, X.; Lian, G.; Liu, Y.; Song, S.; Wang, Q.; Wang, K.; Cui, D. An in-situ surface modification route for realizing the synergetic effect in P3HT-SnO<sub>2</sub> composite sensor and strikingly improving its sensing performance. *Sens. Actuators B Chem.* **2017**, *241*, 1210–1217. [[CrossRef](#)]
42. Saxena, V.; Aswal, D.K.; Kaur, M.; Koiry, S.P.; Gupta, S.K.; Yakhmi, J.V.; Kshirsagar, R.J.; Deshpande, S.K. Enhanced NO<sub>2</sub> selectivity of hybrid poly(3-hexylthiophene): ZnO-nanowire thin films. *Appl. Phys. Lett.* **2007**, *90*, 2005–2008. [[CrossRef](#)]



© 2018 by the authors. Licensee MDPI, Basel, Switzerland. This article is an open access article distributed under the terms and conditions of the Creative Commons Attribution (CC BY) license (<http://creativecommons.org/licenses/by/4.0/>).